A change of the Fermi surface across the metamagnetic transition under pressure in UGe_2

2002 J. Phys.: Condens. Matter 14 L125

(http://iopscience.iop.org/0953-8984/14/5/103)

INSTITUTE OF PHYSICS PUBLISHING JOURNAL OF PHYSICS: CONDENSED MATTER

J. Phys.: Condens. Matter **14** (2002) L125–L135 PII: S0953-8984(02)31971-4

LETTER TO THE EDITOR

A change of the Fermi surface across the metamagnetic transition under pressure in UGe_2

Y Haga[1], M Nakashima[2], R Settai[2,5], S Ikeda[2], T Okubo[2], S Araki[2], T C Kobayashi[3] N Tateiwa[4] and Y Ōnuki[1,2]

[1] Advanced Science Research Centre, Japan Atomic Energy Research Institute, Tokai, Ibaraki 319-1195, Japan
[2] Graduate School of Science, Osaka University, Toyonaka, Osaka 560-0043, Japan
[3] Research Centre for Materials Science at Extreme Conditions, Osaka University, Toyonaka, Osaka 560-8531, Japan
[4] Graduate School of Engineering Science, Osaka University, Toyonaka, Osaka 560-8531, Japan

E-mail: settai@phys.sci.osaka-u.ac.jp

Received 18 December 2001
Published 25 January 2002
Online at stacks.iop.org/JPhysCM/14/L125

Abstract

We have performed the de Haas–van Alphen (dHvA) and ac-susceptibility experiments on a ferromagnet UGe_2 under pressure for the field along the easy a-axis. The p–H phase diagram was determined, indicating three kinds of phase: paramagnetic and weakly and strongly polarized phases. The detected dHvA frequencies as well as the cyclotron masses are found to be very different between the weakly and strongly polarized states. A change of the Fermi surface occurs when the weakly polarized phase is changed into the strongly polarized phase with increasing magnetic field.

(Some figures in this article are in colour only in the electronic version)

The coexistence of superconductivity with magnetism is an important issue in condensed matter physics [1]. In f-electron systems, it was clarified that superconductivity occurs in a quantum critical region where the Néel temperature of antiferromagnets such as $CeIn_3$ and $CePd_2Si_2$ becomes zero [2]. Surprisingly superconductivity was also observed in a ferromagnet, UGe_2, with the Curie temperature $T_C = 52$ K under pressure [3]. This is the first example where superconductivity truly coexists with strong ferromagnetism with a magnetic moment $\mu_s = 1.0\,\mu_B$/U [4,5]. Recently similar superconductivity has been reported at ambient pressure for the ferromagnet URhGe with $\mu_s = 0.42\,\mu_B$/U [6].

UGe_2 crystallizes in the orthorhombic crystal structure of C_{mmm} ($a = 4.0089$ Å, $b = 15.0889$ Å and $c = 4.0950$ Å) with a large lattice constant along the b-axis [7]. The ordered moment μ_s is $1.4\,\mu_B$/U at ambient pressure, directed along the a-axis [8,9]. The b- and c-axes

[5] Author to whom any correspondence should be addressed.

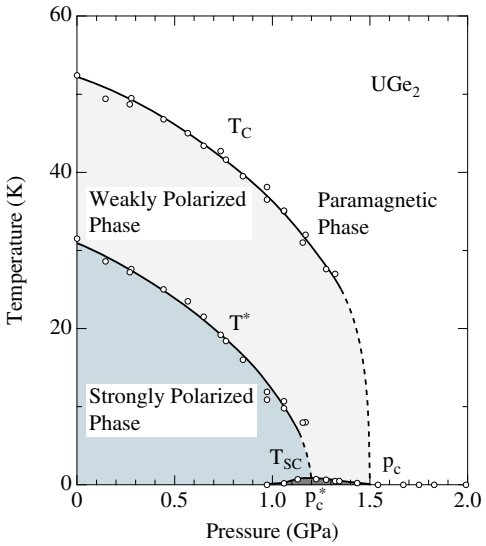

Figure 1. p–T phase diagram in UGe_2. T_C, T^* and T_{SC} mean the Curie temperature, the second phase transition temperature and the superconducting transition temperature, respectively.

are hard axes, indicating strong anisotropy. In the pressure experiment, it was once clarified that with increasing pressure p, T_C (= 52 K) becomes zero roughly at $p_c^* \simeq 2$ GPa [10]. The second phase transition was later found below T_C, at $T^* \simeq 30$ K at ambient pressure [11, 12]. T^* also becomes zero at $p_c^* \simeq 1$ GPa. Around p_c^*, namely in the pressure region from 1.0 to 1.6 GPa, superconductivity was observed below $T_{SC} = 0.7$ K [3]. Figure 1 shows the p–T phase diagram, which was obtained mainly from our resistivity measurement under pressure [5, 13]. Here, $p_c^* \simeq 1.2$ GPa and $p_c \simeq 1.5$ GPa correspond to the critical pressures where T^* and T_C become zero, respectively. The magnetic moment at p_c^* is 1.0 μ_B/U, as mentioned above [4, 14]. The superconducting phase is found around p_c^*, namely within the ferromagnetic phase, and disappears in the paramagnetic region, indicating that the pairing mechanism in superconductivity is ferromagnetic in origin.

It was pointed out that the second phase transition at T^* corresponds to a CDW/SDW formation, although the experimental evidence is not observed yet by the neutron scattering experiment [4, 15]. Experimentally the magnetic moment is enhanced below T^*, which becomes remarkable when pressure approaches p_c^*: from 1.28 to 1.35 μ_B/U at about 0.9 GPa from the neutron scattering experiments [4, 14]. Here the former magnetic moment of 1.28 μ_B/U at about 0.9 GPa is roughly estimated from the temperature dependence of the magnetic moment when the temperature is extrapolated to zero. From the magnetization measurement for the field along the a-axis, the same result was obtained: from 1.18 to 1.26 μ_B/U at 1.18 GPa under the magnetic field of $H = 10$ kOe [14]. The temperature region from T_C to T^* and/or the pressure region from p_c^* to p_c were thus named the weakly polarized phase, while the lower-temperature region ($T < T_C$) and/or the pressure region below p_c^* were named the strongly polarized phase [4, 16].

As mentioned above, the second phase transition at T^* becomes zero at $p_c^* \simeq 1.2$ GPa. When the magnetic field is applied along the a-axis, the weakly polarized phase is changed into the strongly polarized phase at $H = H^*$ even in the pressure region of $p > p_c^*$ [4, 14, 16]. This phenomenon corresponds to the metamagnetic transition, indicating a steplike increase

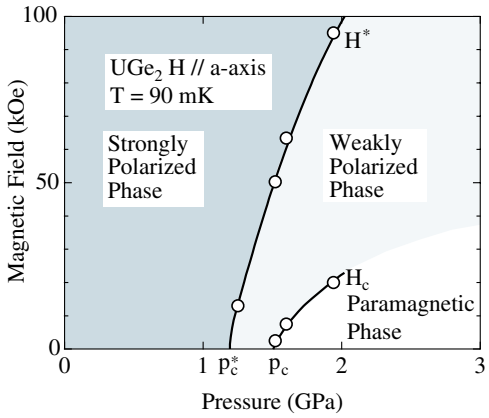

Figure 2. p–H phase diagram for the magnetic field along the a-axis in UGe_2.

of the magnetization curve [14]. This was also reflected in the magnetoresistance and ac susceptibility [4]. The p–H phase diagram for the field along the a-axis is shown in figure 2. The phase boundary from the paramagnetic phase to the weakly polarized phase is also indicated at H_c. These phase boundaries were obtained from the ac-susceptibility measurement, shown later. We note that the metamagnetic transitions occur only for the field along the easy a-axis.

For these peculiar features, the electronic state is an interesting issue to be clarified. The previous de Haas–van Alphen (dHvA) experiment and the energy band calculation indicated that the main Fermi surfaces are highly corrugated but cylindrical along the b-axis [17, 18]. This is mainly due to the flat Brillouin zone along the b-axis. The corresponding cyclotron masses are relatively large, being 15–20 m_0. It was thus concluded that 5f electrons in UGe_2 are itinerant, indicating band magnetism as in the 3d-electron system.

Recent spin-polarized band calculations also indicated similar cylindrical Fermi surfaces [13,19]. The dHvA experiments under pressure for the field along the b-axis indicated that main dHvA branches are clearly observed up to p_c^* but are scarcely seen in the pressure region from p_c^* to p_c [13, 20]. It is, however, remarkable that new dHvA branches with large cyclotron masses $m_c^* \simeq 60m_0$ appear clearly in the paramagnetic region, $p > p_c$. It was suggested from a viewpoint of the Fermi surface property that the phase boundary at p_c is of the first-order phase transition [20]. The recent p–T phase diagram, including our result in figure 1, also indicated that a phase boundary at T_C or p_c is sharp against pressure [21]. This might be also an evidence of a first-order phase transition at p_c. On the other hand, the phase boundary at p_c^* is not clear, most likely of a second-order phase transition. It is important to clarify the reason why the dHvA branches are scarcely seen in the pressure region of p_c^* to p_c, namely in the weakly polarized phase [13].

We have continued carrying out the dHvA experiment under pressure. The present dHvA study under pressure is to clarify the electronic states in both the strongly and weakly polarized phases in figure 2 when the field is directed along the a-axis. We shall discuss a change of the Fermi surface as well as the cyclotron mass and the mean free path when the phase is changed from the weakly polarized phase to the strongly polarized phase at H^*.

The dHvA experiment under pressure was performed by the standard field modulation method with a modulation field of 100 Oe and a modulation frequency of 3.5 Hz in magnetic

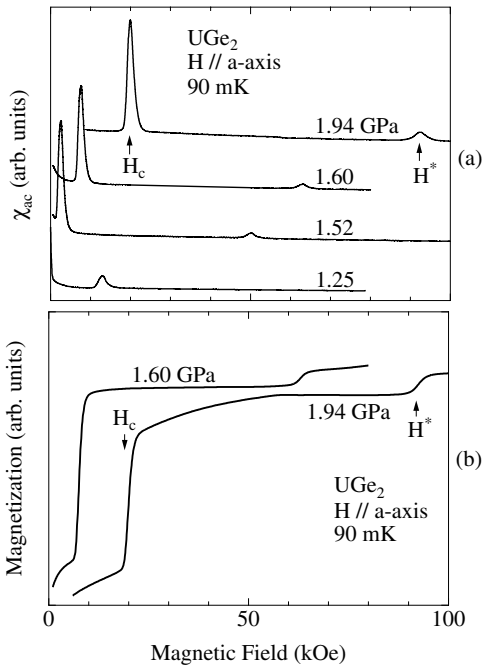

Figure 3. (a) Field dependence of the ac susceptibility for the field along the a-axis under several pressures, and (b) the magnetization curves in UGe_2. H_c and H^* correspond to the phase transitions from the paramagnetic phase to the weakly polarized phase and from the weakly to strongly polarized phases, respectively.

fields up to 170 kOe and at low temperatures down to 90 mK, using an MP35N piston–cylinder cell. The ac-susceptibility χ_{ac} measurement was also carried out using the same dHvA detecting system. The sample was of high quality with a residual resistivity ratio of 500.

Figure 3(a) shows the typical ac susceptibility χ_{ac} under several pressures. For example, the phase transitions occur at $H_c = 20$ kOe and $H^* = 92.5$ kOe at 1.94 GPa. The shape of the transition is different for each. The low-field transition at H_c is sharp compared with the higher-field transition at H^*, which is also reflected in the magnetization curve in figure 3(b), obtained by integrating the ac susceptibility. The absolute magnitude of the magnetization for each pressure is not clear, but most likely reaches 1 μ_B/U at high fields, which might correspond to an ordered moment of 1.0 μ_B/U at $p_c^* \simeq 1.2$ GPa and $H = 0$ kOe. The present experimental data indicate a suggestive result that the phase transition from the paramagnetic phase to the weakly polarized phase is of the first order and the transition from the weakly polarized phase to the strongly polarized phase is of the second order. These transition fields H_c and H^* are thus expressed as a function of pressure, as already shown in figure 2.

Next we show the dHvA data. Figure 4 shows the typical dHvA oscillation and its fast Fourier transformation (FFT) spectrum at ambient pressure. The dHvA frequency $F\ (= \hbar S_F/2\pi e)$ is proportional to the extremal (maximum and minimum) cross-sectional area of the Fermi surface S_F. For the FFT analyses, we took into account the contribution of the magnetic moment M to the effective magnetic field B: $B = H + 4\pi(1 - D)M$. The largest dHvA frequency for branch 'a', shown later, is shifted upward by about 6% by this effect.

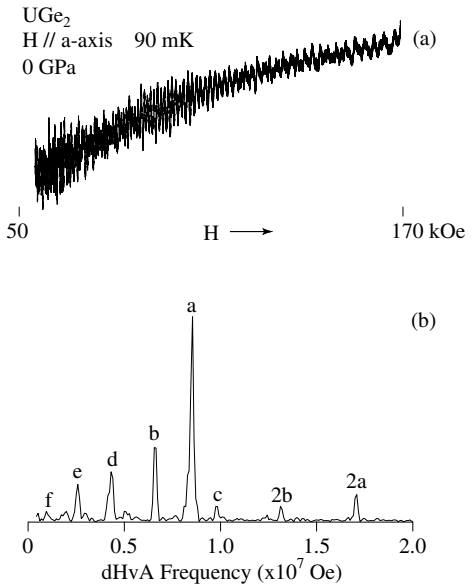

Figure 4. (a) Typical dHvA oscillation at ambient pressure for the field along the a-axis and (b) the corresponding FFT spectrum in UGe_2.

Table 1. dHvA frequency F, cyclotron mass m_c^*, Dingle temperature T_D and mean free path ℓ under 0 and 1.94 GPa in UGe_2.

	$p = 0$ GPa				$p = 1.94$ GPa			
Branch	F ($\times 10^6$ Oe)	m_c^* (m_0)	T_D (K)	ℓ (Å)	F ($\times 10^6$ Oe)	m_c^* (m_0)	T_D (K)	ℓ (Å)
Strongly polarized phase								
a	8.52	4.8	0.42	1100	15.2	7.6	0.34	1150
b	6.61	4.0	0.60	850	14.3			
c	9.80	5.3	0.31	1450				
d	4.34	5.4	0.60	750				
e	2.57	4.2			3.08	5.0		
f	0.97				2.29	3.0		
Weakly polarized phase								
					2.49	11		
					4.16	8.0	0.19	1050

These branches in figure 4 were observed in the strongly polarized phase, as shown in figure 2. All the branches, named 'a, b, c, d, e and f', are almost the same as our previous results [17] and are smaller in cross-section by one order compared with those for the field along the b-axis [13, 20]. This is because the main Fermi surfaces are nearly cylindrical along the b-axis. The origin of the present branches for $H \parallel a$-axis is not clear. We summarize in table 1 the dHvA frequency F, together with the cyclotron mass m_c^*, Dingle temperature T_D and mean free path ℓ for each branch.

Next we show in figure 5 the dHvA oscillation in both the weakly and strongly polarized phases and their FFT spectra at 1.94 GPa. Two dHvA branches are observed in the weakly polarized phase, as shown by arrows, while three or four branches named 'a, b, e and f' are observed in the strongly polarized phase. The dHvA frequencies are very different between the two phases. These results are also summarized in table 1.

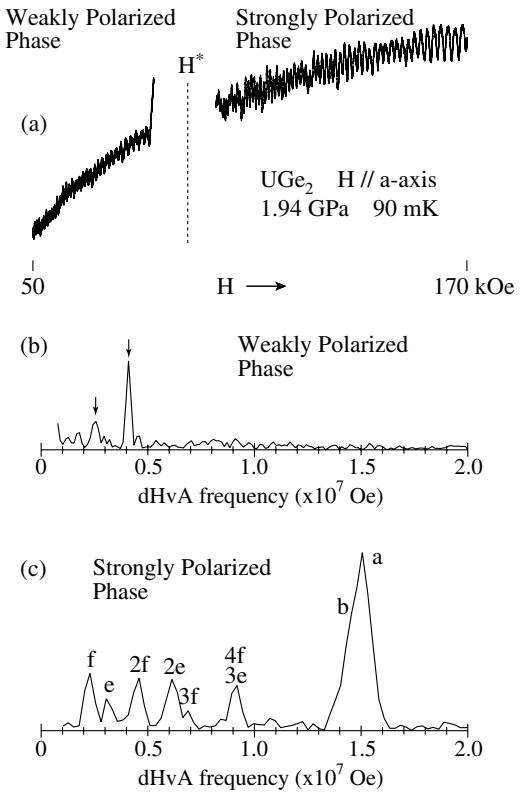

Figure 5. (a) dHvA oscillation at 1.94 GPa for the field along the a-axis and the corresponding FFT spectrum in the (b) weakly and (c) strongly polarized phases of UGe_2.

First we remark the electronic state in the strongly polarized phase. To clarify a change of the dHvA branches, we show in figure 6 the FFT spectra under several pressures, which were measured in the magnetic field from 100 to 170 kOe, namely in the strongly polarized phase. Branch 'c' is observed only at ambient pressure and branch 'd' disappears above about 1 GPa. On the other hand, the other branches are clearly observed up to 1.94 GPa, indicating an increase of the dHvA frequencies with increasing pressure.

Figure 7(a) shows the pressure dependence of the dHvA frequency in both the strongly and weakly polarized phases. The dHvA frequencies of branches 'a, b, e and f' increase with increasing pressure. This result is in contrast with the dHvA result for the field along the b-axis, where the detected main majority up-spin Fermi surfaces shrink in volume with increasing pressure [13, 20]. The present result for $H \parallel a$-axis might suggest that these branches named 'a, b, e and f' correspond to the minority down-spin Fermi surfaces.

In figure 7(b), two kinds of branch with small dHvA frequencies of 2.49×10^6 and 4.16×10^6 Oe in the weakly polarized phase are shown. These branches possess, however, large masses of 11 and 8.0 m_0 at 1.94 GPa, respectively, shown next. When the magnetic field crosses the critical field H^*, the magnetic moment is enhanced. This might bring about a change of the Fermi surface, namely an increase of the volume of the majority up-spin Fermi surfaces. We cannot identify the process by which these small dHvA branches in the weakly polarized phase are connected to those in the strongly polarized phase.

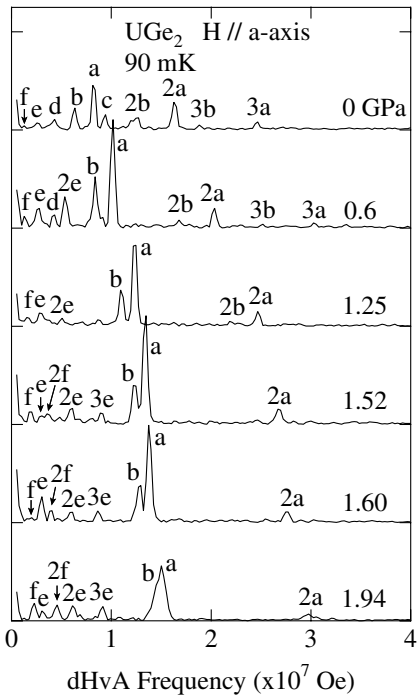

Figure 6. dHvA spectra under several pressures for the field along the *a*-axis in UGe_2.

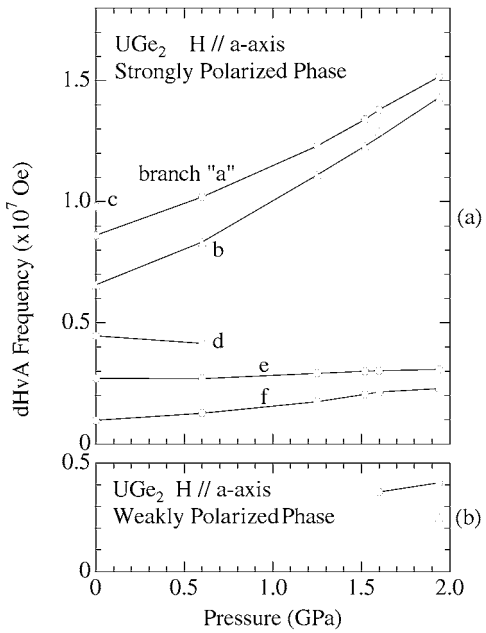

Figure 7. Pressure dependence of the dHvA frequencies in the (a) strongly and (b) weakly polarized phases of UGe_2.

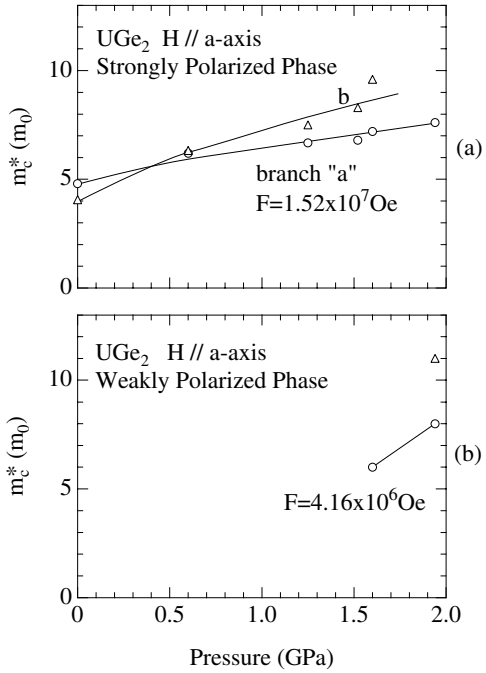

Figure 8. Pressure dependence of the cyclotron mass in the (a) strongly and (b) weakly polarized phases of UGe_2.

Figure 8 shows the corresponding pressure dependence of the cyclotron effective mass m_c^* for each dHvA branch. Here, the cyclotron mass for each branch in the strongly polarized phase was determined from the temperature dependence of the dHvA amplitude in the field range from 100 to 170 kOe. The cyclotron mass increases monotonically with increasing pressure. A large cyclotron mass or large γ value are caused by spin fluctuations, where the freedom of the charge transfer of 5f electrons appears in the form of the 5f-itinerant band, but the freedom of spin fluctuations of the same 5f electrons reveals itself as a ferromagnetic ordering and enhances the effective mass. The cyclotron mass is thus sensitive to the external pressure and also the magnetic field. As mentioned above, the cyclotron masses in the weakly polarized phase, as shown in figure 8(b), are large even though the corresponding dHvA frequencies are small. In general an orbit with a large dHvA frequency possesses a large cyclotron mass. We suppose that the main Fermi surfaces in the weakly polarized phase might have a large mass of about 100 m_0 under the consideration of the γ value and the cyclotron mass in the paramagnetic region [5,13,20]. This is an important result to clarify the reason why the dHvA branches are scarcely seen in the region of p_c^* to p_c, namely in the weakly polarized phase for the field along the b-axis.

We note that the cyclotron mass is field dependent even in the strongly polarized phase. Figure 9 shows the field dependence of the cyclotron mass at 1.25 GPa, close to p_c^*. The cyclotron mass decreases monotonically with increasing field. The mass reduction in fields was reported from the specific heat measurement: $\gamma = 95$ mJ K^{-2} mol^{-1} at $H = 0$ kOe and 50 mJ K^{-2} mol^{-1} at 60 kOe under $p = 1.15$ GPa [22]. The γ value decreases steeply up to about 50 kOe and gradually in higher fields. The present mass reduction in high magnetic fields is consistent with the field dependence of the γ value. We also present in figures 9(b) and (c) the field dependence of the Dingle temperature T_D and the mean free path ℓ. The T_D

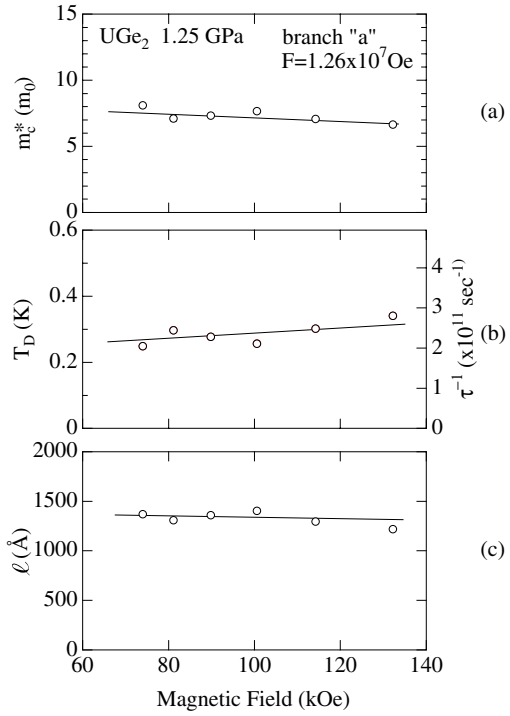

Figure 9. Field dependence of the cyclotron mass, Dingle temperature and mean free path for branch 'a' at 1.25 GPa in the strongly polarized phases of UGe_2.

value increases slightly with increasing field but the mean free path of $\ell = 1300$ Å is not field dependent. Here, T_D $(= \hbar/2\pi k_B \tau)$ is inversely proportional to the scattering lifetime of the conduction electron τ. The mean free path ℓ was estimated from the dHvA frequency F, the cyclotron mass m_c^* and the Dingle temperature T_D : $S_F = \pi k_F^2$, $\hbar k_F = m_c^* v_F$ and $\ell = v_F \tau$, where k_F is half of the caliper dimension of circular S_F and v_F is the Fermi velocity.

Finally we compare the electronic phase in the weakly polarized phase with that in the strongly polarized phase. As indicated above, the dHvA frequency is very different between the two phases. Figure 10 shows the field dependence of the cyclotron mass m_c^*, the Dingle temperature T_D and the mean free path l at 1.94 GPa. The dHvA frequency of 4.16×10^6 Oe in the weakly polarized phase indicates a decreasing tendency of the cyclotron mass with increasing magnetic field. The similar field dependence of m_c^* is also detected for branch 'a' in the strongly polarized phase. The mean free path is almost the same between the two phases: about 1000 Å for $F = 4.16 \times 10^6$ Oe in the weakly polarized phase and for branch 'a' ($F = 1.52 \times 10^7$ Oe) in the strongly polarized phase.

We summarize our experimental results. In the present experiments we determined the p–H phase diagram for the field along the a-axis. Two metamagnetic transitions were observed at H_c and H^* in the pressure region of $p > p_c$, where the paramagnetic phase, the weakly polarized phase and the strongly polarized phase appear successively with increasing magnetic field. The dHvA frequency is very different between the weakly and strongly polarized phases, although the corresponding cyclotron masses decrease with increasing magnetic field.

In the strongly polarized phase, some detected dHvA frequencies increase with increasing pressure. These branches might correspond to the minority down-spin Fermi surfaces.

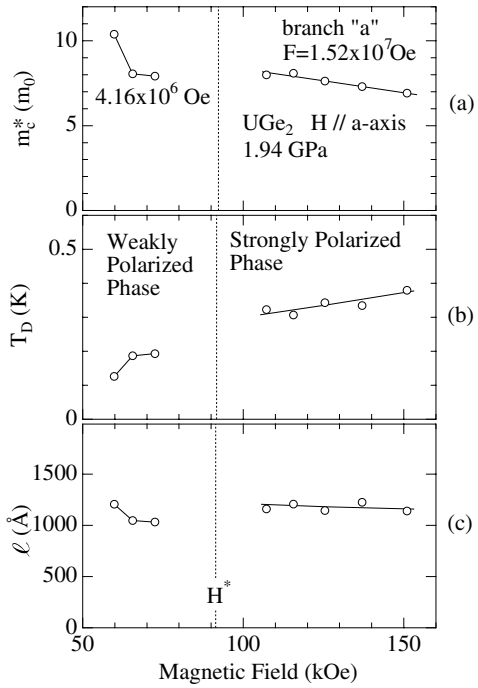

Figure 10. Field dependence of the cyclotron mass, Dingle temperature and mean free path for the branch with $F = 4.16\times10^6$ Oe in the weakly polarized phase and branch 'a' with $F = 1.52\times10^7$ Oe in the strongly polarized phase at 1.94 GPa in UGe_2.

Unfortunately main Fermi surfaces were not observed for the field along the a-axis because the main Fermi surfaces are highly corrugated but cylindrical along the b-axis. On the other hand, we detected two dHvA branches in the weakly polarized phase, although these branches have much smaller dHvA frequencies, namely much smaller cross-sections of Fermi surfaces than those in the strongly polarized phase. We could not identify the process by which these dHvA branches in the weakly polarized phase are connected to those in the strongly polarized phase. This result might claim that the main dHvA branches in the strongly polarized phase are not smoothly connected to those in the weakly polarized phase when pressure crosses p_c^* for the magnetic field along the b-axis.

The dHvA branches with the small dHvA frequencies in the weakly polarized phase possess, however, large cyclotron masses compared with those with the similar dHvA frequencies in the strongly polarized phase, as shown in table 1. This result also claims that the main Fermi surfaces in the weakly polarized phase, which are not detected for the field along the a-axis, should possess a large cyclotron mass of 100 m_0. This is most likely a main reason why the dHvA branches for the field along the b-axis are scarcely seen in the pressure region of p_c^* to p_c, namely in the weakly polarized phase. We note that the mean free path is almost the same between the two phases. It is important to detect the main Fermi surfaces in the weakly polarized phase for the field along the b-axis. Further experiments are in progress.

We are grateful to Professor K Miyake for helpful discussion. This work was supported by the Grant-in-Aid for Scientific Research COE (10CE2004) from the Ministry of Education, Culture, Science, Sports and Technology.

References

[1] Sigrist M and Ueda K 1991 *Rev. Mod. Phys.* **63** 239
[2] Mathur N D, Grosche F M, Julian S R, Walker I R, Freye D M, Haselwimmer R K W and Lonzarich G G 1998 *Nature* **394** 39
[3] Saxena S S *et al* 2000 *Nature* **604** 587
[4] Huxley A, Sheikin I, Ressouche E, Kernavanois N, Braithwaite D, Calemczuk R and Flouquet J 2001 *Phys. Rev.* B **63** 144519
[5] Tateiwa N, Kobayashi T C, Hanazono K, Amaya K, Haga Y, Settai R and Ōnuki Y 2001 *J. Phys.: Condens. Matter* **13** L17
[6] Aoki D, Huxley A, Ressouche E, Braithwaite D, Flouquet J, Brison J P, Lhotel E and Paulsen C 2001 *Nature* **413** 613
[7] Oikawa K, Kamiyama T, Asano H, Ōnuki Y and Kohgi M 1996 *J. Phys. Soc. Japan* **65** 3229
[8] Menovsky A, de Boer F R, Frings P H and Franse J J M 1983 *High Field Magnetism* ed M Date (Amsterdam: North-Holland) p 189
[9] Ōnuki Y, Ukon I, Yun S W, Umehara I, Satoh K, Fukuhara T, Sato H, Takayanagi H, Shikama M and Ochiai A 1992 *J. Phys. Soc. Japan* **61** 293
[10] Takahashi H, Môri N, Ōnuki Y and Yun S W 1993 *Physica* B **186–8** 772
[11] Oomi G, Nishimura K, Ōnuki Y and Yun S W 1993 *Physica* B **186–8** 758
[12] Oomi G, Kagayama T, Nishimura K, Yun S W and Ōnuki Y 1995 *Physica* B **206–7** 515
[13] Settai R, Nakashima M, Araki S, Haga Y, Kobayashi T C, Tateiwa N, Yamagami H and Ōnuki Y 2002 *J. Phys.: Condens. Matter* **14** L29
[14] Tateiwa N *et al* 2001 *J. Phys. Soc. Japan* **70** 2876
[15] Watanabe S and Miyake K 2001 *SCES '2001 (Ann Arbor) Physica* B at press
[16] Huxley A, Sheikin I and Braithwaite D 2000 *Physica* B **284–8** 1277
[17] Satoh K, Yun S W, Umehara I, Ōnuki Y, Uji S, Shimizu T and Aoki H 1992 *J. Phys. Soc. Japan* **61** 1827
[18] Yamagami H and Hasegawa A 1993 *Physica* B **186–8** 182
[19] Shick A B and Picket W E 2001 *Phys. Rev. Lett.* **86** 300
[20] Terashima T, Matsumoto T, Terakura C, Uji S, Kimura N, Endo M, Komatsubara T and Aoki H 2001 *Phys. Rev. Lett.* **87** 166401
[21] Bauer B D, Dickey R P, Zapf V S and Maple M B 2001 *J. Phys.: Condens. Matter* **13** L759
[22] Tateiwa N, Kobayashi T C, Hanazono K, Amaya K, Haga Y, Settai R and Ōnuki Y 2001 *SCES '2001 (Ann Arbor) Physica* B at press